Glaciation at Euripus Mons, Mars: Insights from combining numerical ice flow modeling, SHARAD observations and high-resolution topography Reid Parsons[1], John W. Holt[2], [1]NASA Ames Research Center, (reid.a.parsons@nasa.gov) [2]Institute for Geophysics, University of Texas at Austin

Introduction: Radar sounding of Lobate Debris Aprons (LDAs) by the SHARAD instrument on MRO has led to the discovery that these deposits are ice-rich (no more than a few tens of percent solid particles by volume) and range in thickness from 300 to 700 m [1,2]. These observations can be used to constrain the rheology of LDA ice through the comparison of numerical ice flow simulations with the LDA topography [3]. Such comparisons can potentially assess the age, basal topography, and climate conditions under which LDAs formed. However, given the number of factors that influence the topographic shape of martian ice deposits, numeric models need to be tailored to the topographic setting of specific deposits in order to account for converging/diverging flow [4], basal slope, and flux of ice from the headward catchment. Even after considering these factors, the spatial and temporal pattern of precipitation and ablation may give non-unique solutions.

In order to better assess the influence of these factors on LDA topography, we are currently incorporating them into an existing ice flow model [3]. Comparing future flow model results to both the surface and basal topography (using HRSC, MOLA and SHARAD data) will provide insight into subsurface geometry, ice rheology, accumulation history, and, by extension, the past climate conditions responsible for the deposition of LDA ice.

Observations: Debris apron complexes consisting of a single apron or, more commonly, a laterally extensive mass of multiple, coalesced aprons derived from a common source are found in several distinct regions on Mars - such as Deuteronilus Mensae, eastern Hellas, and Argyre basin. Here, we focus on Euripus Mons, located to the east of Hellas basin where a 4 km high mountain is surrounded by a 20 km wide LDA deposit as indicated by the MOLA and HRSC topography in Fig. 1a. The green line in Fig. 1a gives the drainage divide associated with one section of the LDA based on HRSC topography (overlain hillshade). CTX imagery of the LDA surface (Fig. 1b, from black box in (a)) exhibits compression folds (black arrows) and sublimation pitting (white arrow) characteristic of flowing ice. HRSC (image 2345_0000) contours are overlain at 200 m intervals at a spatial resolution of 75 m/px. The depth corrected SHARAD radar profile [1] along B to B′ is shown in Fig. 1c showing the surface return (dashed line) and a subsurface reflection (arrow).

Flow Modeling: Our glacial flow model simulates changes in ice thickness as ice flows outward over a flat or sloping surface in 1-D while accounting for influences from ice grain size, temperature, dust fraction, and the magnitude of the applied differential stress in driving

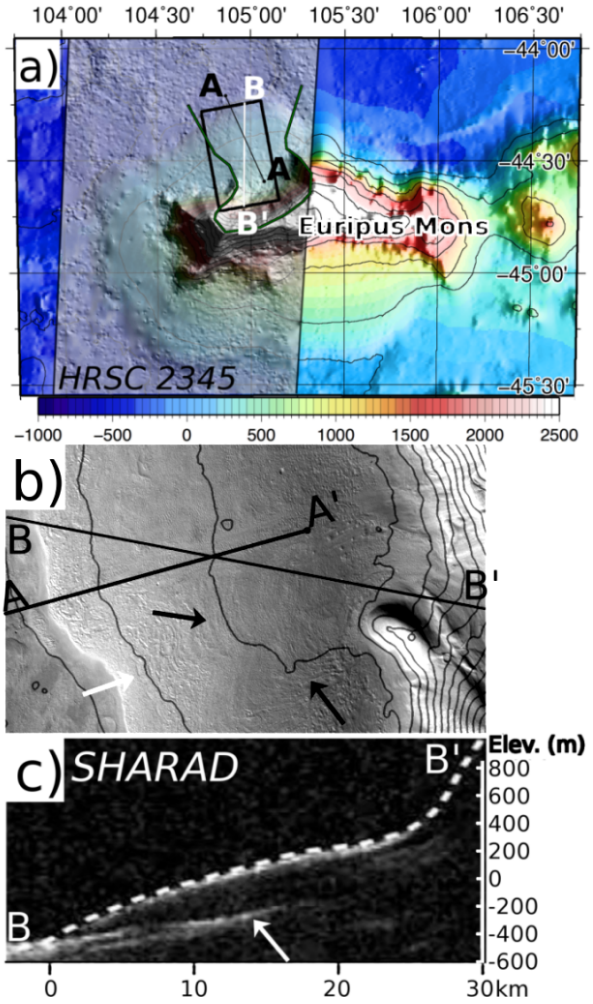

Figure 1: Topographic, visible, and radar observations of an LDA at Euripus Mons. a) MOLA shaded relief contour (500 m interval) with overlain HRSC hillshade. b) CTX image (black box in (a)) of the LDA surface which exhibits compression folds (black arrows) and sublimation pitting (white arrow). HRSC topographic contours (200 m interval) are overlain. c) Depth-corrected version of SHARAD radargram (from *Holt et al., 2008* for the B-B profile showing the surface return (dashed line) and a subsurface reflection (arrow). HRSC topography along A-A′ is shown in Fig. 2.

viscous deformation. In contrast to most previous martian ice flow models which utilize an ice rheology from Glens Flow Law, this model incorporates data from more recent ice deformation experiments which show a change in the the rheology of ice at different applied stresses and ice grain sizes [5]. The shear stress at the base of an ice sheet and the resultant strain rate are

$$\tau = \rho g(h-z)\left(\frac{\partial h}{\partial x} + \sin\theta\right) \quad (1)$$

$$2\dot{\epsilon} = \frac{\partial v}{\partial z} = 2A\tau^n d^{-p} \quad (2)$$

where v is the velocity in the x direction, n is the stress exponent, d is the ice grain size, ρ is the ice (or ice-dust mixture) density, g is gravity, and θ is the basal slope. The quantities z and x are the slope-perpendicular and downslope coordinate directions, respectively, and $z = 0$ at the base of the ice.

Three different ice creep regimes have been identified, which range from diffusion, to grain size-sensitive (GSS), to dislocation creep with increasing stress. The dependence of strain rate on the applied stress and grain size through the values of n and p is a function of the creep regime. For 500 m thick ice sheets on Mars, the dominant ice deformation mechanism is GSS creep (n =2) [3]. A is a temperature- and dust fraction-dependent flow parameter

$$A = A' e^{\left(\frac{-Q}{RT} - b\phi\right)} \quad (3)$$

where A' is equal to 5×10^{-15} Pa^{-2} s^{-1} (fitted to *Goldsby and Kohlstedt (2001)*) for GSS creep. Q is the activation energy, T is the ice temperature, ϕ is the dust volume fraction, and b =2.9 is a constant [6-8] at $\phi <$ 55% where the rheology of the dust-ice mixture is not dominated by interactions between solid particulates [7].

Using the above equations, we can determine the change in ice thickness of an initial ice sheet for in the GSS (n=2) creep regime by first combining and integrating Eqs. (1) and (2) to calculate the horizontal velocity, and then apply the 2D Cartesian continuity equation (see [9]) to give:

$$\frac{\partial h}{\partial t} = \frac{1}{2} A' d^{-p} \rho^2 g^2 \frac{\partial}{\partial x}\left[h^4 \left(\frac{\partial h}{\partial x} + \sin\theta\right)\right] e^{\frac{-Q}{RT} - b\phi} \quad (4)$$

The important variables to explore are: ice temperature (T), duration of ice flow, basal slope, and dust volume fraction (ϕ). The model assumes that T and $\phi$are spatially homogeneous within the ice deposit. Eqn. (4) assumes a laterally and vertically constant temperature which is appropriate because we are most concerned with the basal portion of the LDA deposit where most of the deformation takes place, and conduction produces little temperature variation over this basal layer. In the preliminary simulations shown here, flow convergence/divergence is neglected (constant width) as is precipitation and ablation, as we focus on the effect of a basal slope on the topography of LDAs.

Results & Implications: A simple example of the predictions made by the ice flow model is shown in Fig. 2. We varied only the basal slope between two simulations with T = 205 K and d = 1 mm while neglecting flow convergence/divergence. The simulated topographic profiles in part (a) (dashed lines) plot distance from the toe of the LDA versus elevation. The initial ice deposit is plotted toward the right for both simulations as well as the profile after 20 Myrs of flow over a flat (thick, gray, lines) or 1° sloping surface (thin, black lines). The red line is the topographic profile from A to A′ observed by HRSC and the black dots give the basal topography as seen by SHARAD (derived from data shown in Fig. 1c). Note that flow over a flat surface does not produce as good a fit to the observed topography as does flow over a 1° sloping surface. The prediction of the presence of a basal slope by the model is in agreement with SHARAD data as indicated by the overlap between the black dots and the solid black line representing the basal slope in Fig. 2a. A comparison of the observed surface slope (averaged over a 375 m moving window) to the final state of these two simulations is shown in Fig. 2b. The modeled topography is not an excellent fit to the data for even the sloping subsurface case, which suggests modification by sublimation and/or mass wasting at the toe of the deposit has taken place. A better fit may result from incorporating the effect of flow convergence and divergence. Also, the fast timescale in these simulations suggests that a higher viscosity (larger ice grain size) may give better results. Future simulations will address these issues at Euripus Mons and elsewhere.

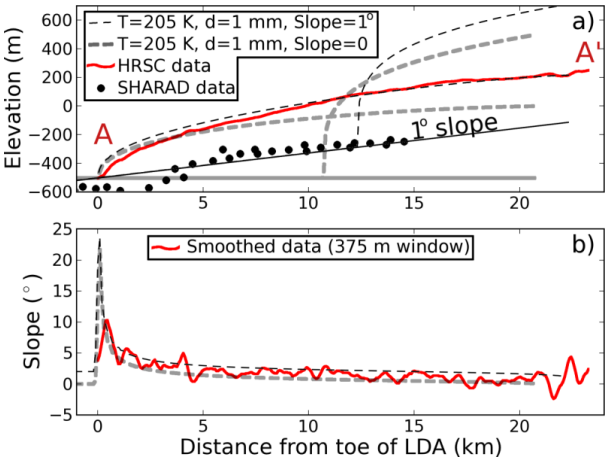

Figure 2: Comparison of model results to topographic and radar observations of an LDA at Euripus Mons. a) The thick red line is an HRSC topographic profile (labelled A-A in Fig. 1a) and the dashed lines give the initial ice deposits and after 20 Myrs of flow (T = 205 K, d =1 mm) over a flat (thick, gray lines) and 1° sloping surface (thin, black lines). Elevation points from the basal interface radargram (Fig. 1c) are shown as gray dots - confirming the models indication of a nonzero basal slope. b) Observed slope (375 m moving window average) compared to the 20 Myr simulations (red and dashed lines, respectively.

References: [1] Holt, J., et al. (2008), Science, 322, 12351238. [2] Plaut, J., et al. (2009), Geophys. Res. Lett. 36. [3] Parsons, R. A., et al. (2011), Icarus, 214, 246257. [4] Winebrenner, D.P., et al. (2008), Icarus, 195, 90-105. [5] Goldsby, D.L. & Kohlstedt, D.L. (2001), J. Geophys. Res., 106, 11,017-11,030. [6] Goughnour, R. & Andersland, O. (1968), Soil Mech. Found. Div., 923950. [7] Durham, W., et al. (1992), J. Geophys. Res., 97, 20,88320,897. [8] Mangold, N., et al. (2002). Planet. Space Sci. 50, 385401. [9] Patterson, W., (1994). Physics of Glaciers, third ed. Elsevier.